Atomic transport in ordered compounds mediated by local disorder: Diffusion in $B2$-Ni_xAl_{1-x}

Qingchuan Xu and Anton Van der Ven
Department of Materials Science and Engineering, The University of Michigan, Ann Arbor, Michigan 48109, USA
(Received 11 January 2010; published 26 February 2010)

Although $B2$-NiAl has one of the simplest crystal structures of any intermetallic compound, its atomic transport mechanisms are complex and remain poorly understood. Here, we report on a first-principles study of diffusion in $B2$-NiAl that simultaneously accounts for all relevant hop mechanisms in kinetic Monte Carlo simulations. Diffusion in $B2$-NiAl occurs not only through first- and second-nearest-neighbor hops, but also through simultaneous pair-atom hops with the dominant transport mechanism being very sensitive to the bulk alloy concentration and degree of local disorder.

DOI: 10.1103/PhysRevB.81.064303 PACS number(s): 66.30.−h, 61.72.Bb

The $B2$-CsCl crystal structure [Fig. 1(a)] is among the simplest ordered arrangements of two components on a bcc lattice and is formed by many important intermetallic compounds including NiAl. The simplicity of many of these compounds ends with their crystal structure, however. $B2$-NiAl, for example, is able to tolerate large deviations in composition from the ideal (50/50)% stoichiometric composition, exhibiting vacancy concentrations on the Ni sublattice up to 15% when Al-rich and similar concentrations of Ni-antisite atoms (excess Ni occupying the Al sublattice) in Ni-rich alloys.[1–3] These high concentrations of point defects play a crucial role in mediating atomic diffusion, an important property from technological and fundamental points of view that has preoccupied materials scientists for over 50 years.[4–9] A variety of hop mechanisms and cyclic hop sequences have been proposed in $B2$-NiAl (Refs. 4 and 6–8); however, no consensus has been reached as to the dominant hop mechanisms responsible for diffusion. One impediment to achieving a fundamental understanding of diffusion in $B2$-NiAl is that no Al isotopes are readily available, preventing a direct measurement of Al tracer diffusion coefficients.

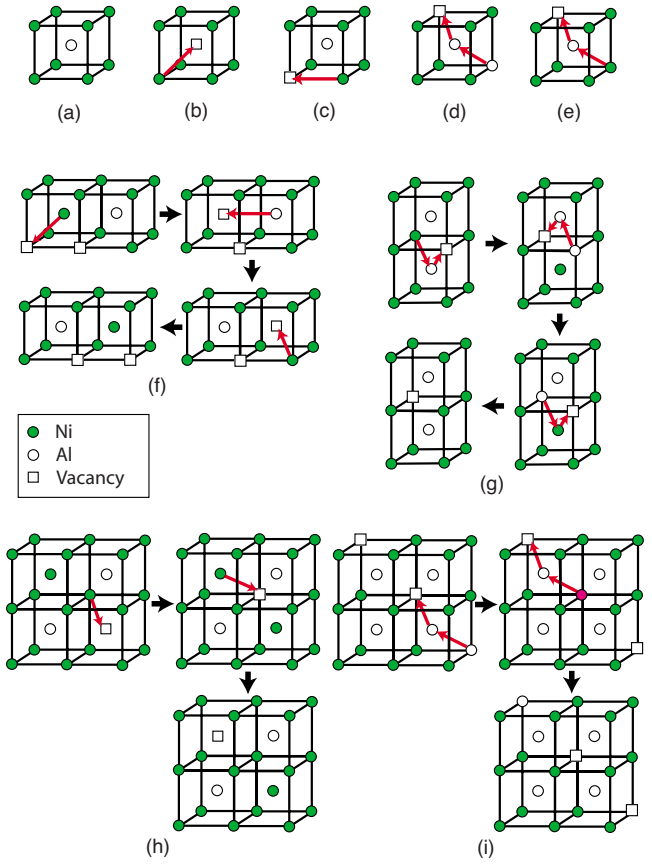

FIG. 1. (Color online) (a) $B2$ crystal structure, (b) nearest-neighbor hop, (c) next-nearest-neighbor hop, (d) SPA hop involving two Al atoms, (e) SPA hop involving one Ni atom and one Al atom, (f) triple-defect sequence, (g) six-jump-cycle sequence (involving a sequence of three simultaneous pair-atom hops), (h) ASB sequence for Ni atoms, and (i) ASB sequence for Al atoms.

Diffusion in typical metallic alloys is mediated by a dilute concentration of vacancies that stochastically wander throughout the crystal.[10–12] Analytical expressions for diffusion coefficients have been derived for thermodynamically ideal alloys.[10,13–15] $B2$-NiAl, however, is an ordered compound, deviating far from thermodynamic ideality and exhibiting an unusually high concentration of vacancies. In fact, the high vacancy concentration on the Ni sublattice of Al-rich $B2$-NiAl is reminiscent of intercalation compounds used as electrodes in Li-ion batteries. Li diffusion in these compounds occurs in the nondilute regime by exchanging with neighboring vacant interstitial sites.[16,17] Although Ni second-nearest-neighbor hops in $B2$-NiAl resemble diffusion in intercalation compounds as these hops keep Ni on its own sublattice, several viable hop cycles proposed in past decades involve exchanges between Al and Ni of the two sublattices.[4,6–8] Furthermore, experiment indicates that the Al mobility is also sizable in $B2$-NiAl (Ref. 9) in spite of the fact that the concentration of vacancies on the Al sublattice is very low.[2,3] Diffusion in $B2$-NiAl is therefore quite distinct from what is known to occur in metallic solid solutions and in more complex systems such as intercalation compounds.

Here, we simultaneously incorporate the most important hop mechanisms of $B2$-NiAl within a kinetic Monte Carlo (kMC) framework and predict tracer diffusion coefficients from first principles. The results show that the dominant hop mechanisms in $B2$-NiAl are very sensitive to small changes in alloy concentration and are enhanced by local disorder.

A complicating factor in studying diffusion in $B2$-NiAl is that the concentration of its diffusion mediating point defects is unusually high for a metallic phase and any rigorous treatment of their thermodynamic and kinetic behavior must explicitly account for interactions among point defects. We re-

cently developed a first-principles lattice model Hamiltonian (based on the cluster expansion formalism[18]) for the $B2$-NiAl system that accounts for interactions among antisite point defects and vacancies.[3] The cluster expansion was parametrized by fitting to first-principles energies, calculated with approximations to density-functional theory (DFT) of 175 different point-defect configurations within $B2$-NiAl.[3] The DFT calculations were performed with the VASP code[19,20] in the generalized gradient approximation (GGA) using the projector augmented wave (PAW) method.[21,22] The predicted point-defect concentrations from grand canonical Monte Carlo (MC) simulations applied to the cluster expansion show,[3] in agreement with experiment,[1] that excess Al in Al-rich $B2$-NiAl is accommodated by the introduction of high concentrations of vacancies on the Ni sublattice, while excess Ni in Ni-rich $B2$-NiAl is accommodated by Ni-antisite atoms on the Al sublattice. Although vacancies on the Al sublattice and Al-antisite atoms on the Ni sublattice are also predicted, their concentrations are significantly lower than the dominant defects of Ni vacancies and Ni-antisite atoms.[2,3] The Monte Carlo simulations also predict the existence of defect complexes such as triple defects, which consist of pairs of Ni vacancies (i.e., vacancies on the Ni sublattice) clustered around a Ni-antisite atom.[3]

Many hop mechanisms have been proposed for $B2$-NiAl based on experimental and theoretical considerations.[4,6–8] In addition to nearest-neighbor (NN) hops, next-nearest-neighbor (NNN) hops are also viable in $B2$-NiAl due to its open crystal structure. An intriguing property of $B2$-NiAl is that NN Al hops from the Al sublattice to the Ni sublattice cannot occur as the end state is predicted to be mechanically unstable.[3,8] A mechanism with which Al is able to migrate to the Ni sublattice is then through a simultaneous pair-atom (SPA) hop as illustrated in Figs. 1(d) and 1(e) involving either an Al-Ni pair or an Al-Al pair hopping into a Ni vacancy.[3,8,23] With the exception of NNN hops, the NN hops and simultaneous pair-atom hops result in local disordering of $B2$, necessitating hop cycles, such as the six-jump cycle (6JC),[4] to restore $B2$ ordering. Recent DFT calculations have shown that the 6JC is in fact a three-jump cycle involving only simultaneous pair-atom hops[8,23] [Fig. 1(g)]. Cyclic hop mechanisms have also been proposed for the net migration of defect complexes such as the triple defect.[7] First-principles calculations have predicted that a triple defect migrates through a NN Ni hop, followed by a NNN Al hop and completed by a NN Ni hop[3,23] [Fig. 1(f)].

The frequency Γ with which an elementary hop occurs can be accurately estimated with transition state theory according to $\Gamma = \nu^* \exp(-\Delta E_B / k_B T)$, where the vibrational prefactor ν^* and the migration barrier ΔE_B can be calculated with DFT.[24] For consistency purposes, we have calculated the migration barriers and vibrational prefactors (within the local harmonic approximation[25]) for all elementary hop mechanisms (NN, NNN, and pair-atom hops involving Al-Al and Al-Ni pairs) in different local environments characterizing typical states of local disorder in $B2$-NiAl within the GGA approximation to DFT (details can be found in the Appendix).

To evaluate the relative importance of the various hop mechanisms in mediating atomic transport in $B2$-NiAl, we

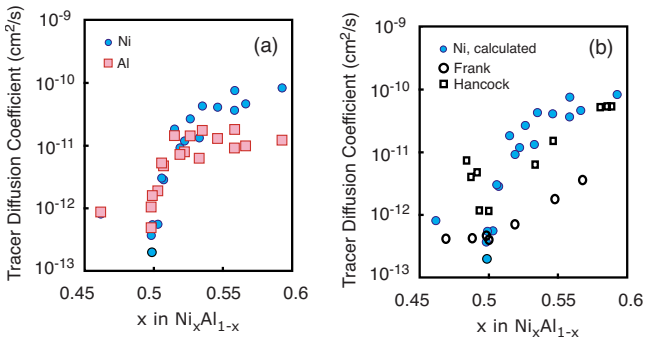

FIG. 2. (Color online) (a) Calculated tracer diffusion coefficients for Ni (circles) and Al (squares) at 1300 K. (b) Comparison of calculated (1300 K, filled circles) and experimental Ni tracer diffusion coefficients. Squares at ~1273 K (Ref. 5) and circles at 1300 K (Ref. 7).

developed a kMC code that accounts for the energies of the end states of atomic hops (using our cluster expansion for $B2$-NiAl)[3] and that incorporates all possible NN and NNN hops as well as simultaneous pair-atom hops (Al-Ni and Al-Al pairs) into vacancies on the Ni sublattice (nearest-neighbor Al hops were forbidden in the kMC simulations as they result in mechanically unstable end states according to DFT). To account for the environment dependence of the migration barriers, we used an approach described in Ref. 16, in which a kinetically resolved activation (KRA) barrier is introduced for each hop, defined as an averaged barrier over back and forth hops. The actual barrier for a particular hop can then be reconstructed by adding the KRA barrier to the average energy of the end states of the hop, calculated with the cluster expansion, minus the energy of the initial state.[16] The KRA barriers are sensitive to any local disorder that may be present. Within our kinetic Monte Carlo simulations we tabulated KRA barriers for each elementary hop and for different local environments as determined by the occupancy in sites that are within the nearest-neighbor shell of any of the sites participating in the hop. (While this is a shorter range than that of the cluster expansion for the end states, it is, nevertheless, reasonable to expect that variations of the activated state energy with environment should be closely correlated with the initial- and final-state energies.) This approach ensures that the concentrations of point defects and defect clusters within the kinetic Monte Carlo simulations are representative of those in thermal equilibrium (since the energies of the end states of the hop are calculated with the cluster expansion) and that the effect of any variations in composition and disorder on hop mechanisms and barriers are accurately accounted for.

Kinetic Monte Carlo simulations[26] allow us to sample representative atomic trajectories for the evaluation of tracer diffusion coefficients, defined as $D_i^* = \langle \Sigma_\xi [\Delta \vec{R}_\xi^i(t)]^2 \rangle / 6tN_i$, where $\Delta \vec{R}_\xi^i(t)$ is the vector linking the end points of the trajectory of atom ξ of type i (Ni or Al) after time t. N_i refers to the number of atoms of type i while the angular brackets correspond to an ensemble average.

Figure 2 illustrates predicted tracer diffusion coefficients for both Ni and Al as functions of bulk alloy concentration [defined as $x_{\mathrm{Ni}}/(x_{\mathrm{Ni}}+x_{\mathrm{Al}})$, where x_i refers to the fraction of

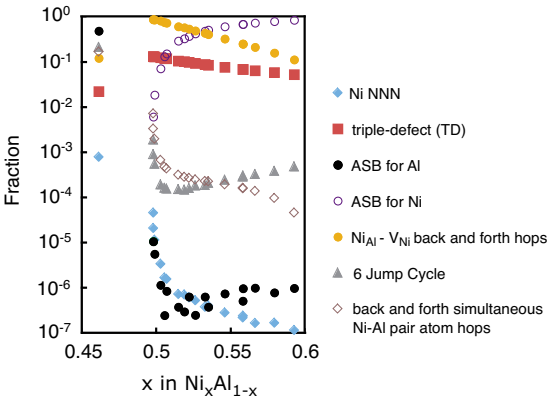

FIG. 3. (Color online) Decomposition of hop mechanisms and sequences as functions of alloy composition at 1300 K.

bcc sites occupied by specie i] calculated at 1300 K. As is evident from Fig. 2(a), the predicted tracer diffusion coefficients depend strongly on composition, exhibiting a minimum at stoichiometric NiAl. In Ni-rich alloys, the Ni tracer diffusion coefficient is larger than that of Al. In Al-rich alloys, however, the tracer diffusion coefficients of Ni and Al are very similar, in spite of the fact that the Ni sublattice has a high concentration of vacancies. Although experimental Al tracer diffusion coefficients are not available, several measurements of Ni tracer diffusion coefficients have been performed.[5,7] The measurements of Hancock and Mcdonnel[5] and Frank *et al.*[7] qualitatively exhibit similar trends with alloy composition as predicted here; however, they quantitatively differ from each other by as much as an order of magnitude in Al- and Ni-rich alloys [Fig. 2(b)]. Both measured an increase in the Ni tracer diffusion coefficient with increasing Ni concentration above stoichiometric NiAl. The Ni tracer diffusion coefficient measured by Hancock and Mcdonnel[5] exhibits a pronounced minimum at the stoichiometric NiAl composition, while that measured by Frank *et al.*[7] remains constant as the alloy becomes Al rich.

A unique advantage of the kinetic Monte Carlo simulations is that it allows us to track the frequency with which the various hops occur as functions of alloy composition, thereby providing insight about the dominant diffusion mechanisms responsible for atomic transport in $B2$-NiAl (Fig. 3). Fractions for cyclic hop mechanisms (i.e., 6JC and triple defect) and hop sequences are based on estimates of the sum of the total number of subhops making up the sequence (see the Appendix for details).

Around stoichiometry, the most frequent hop sequences are Ni-antisite/Ni-vacancy back and forth hops due to its relatively low migration barrier (~0.7 eV averaged over the back and forth hop directions[3]). These hops, however, do not contribute to macroscopic transport (and therefore to D^*_{Ni}) since a back and forth hop restores the Ni atom to its initial position. The next most frequent hop mechanism at stoichiometry is the triple-defect hop sequence in which a Ni antisite next to a pair of Ni vacancies performs a sequence of three hops [Fig. 1(f)] that result in a net migration of the triple defect by a cubic lattice parameter. As the Ni concentration of the alloy is increased above stoichiometry, the dominant hop mechanism changes to the anti-structure-bridge (ASB) mechanism,[6] whereby vacancies—which energetically prefer the Ni sublattice—can migrate along percolating networks of nearest-neighbor Ni chains connected by Ni-antisite atoms. Since the existence of the percolating networks requires Ni-antisite atoms, the ASB sequence is only viable in Ni-rich alloys where off stoichiometry is accommodated by Ni-antisite atoms.[6] The average migration barrier for Ni-NN hops is comparatively low (~0.7 eV) and the migration of a vacancy along a percolating network of Ni-antisite atoms does not result in any increased disorder, thereby making the ASB sequence a very effective mechanism to transport Ni atoms. As a result, while Al predominantly migrates by means of the triple-defect mechanism, the Ni atoms can migrate via both the triple-defect and the ASB mechanisms resulting in a Ni tracer diffusion coefficient exceeding that of Al above a threshold composition upon which the percolating NN Ni pairs consisting of Ni-antisite atoms are formed.

In Al-rich alloys (only one concentration was considered in Al-rich $B2$-NiAl as very large Monte Carlo cells are required to ensure that the equilibrium concentrations for Al antisite atoms, Ni antisite atoms, and Al vacancies are present), the dominant diffusion mechanisms change again, with the triple-defect mechanism becoming less important and the ASB sequence involving Ni no longer viable. Instead Ni and Al transport is mediated by the 6JC (which are in fact a sequence of three simultaneous pair-atom hops) and what we will refer to as the Al-ASB sequence. Also very high in Al-rich alloys are back and forth simultaneous Ni-Al pair hops, but they do not contribute to long-range atomic transport. The 6JC, while having high migration barriers for the first hop (above 2.3 eV),[3,8,23] becomes a dominant mechanism in Al-rich alloys due to the large concentration of Ni vacancies. Its high frequency has an entropic origin as there are 48 symmetrically equivalent pair-atom hops that can initiate the 6JC sequence for each Ni vacancy. An important result in Fig. 3 is that Ni NNN hops are not significant at any composition, even in Al-rich alloys where the Ni-vacancy concentration is very high. This is in large part due to its high migration barrier (~2.7 eV) and the fact that only six NNN hops are possible for a Ni vacancy.

The other dominant diffusion mechanism in Al-rich alloys involves pair-atom hops in which an Al on the Al sublattice and an antisite Al simultaneously hop into a Ni vacancy. This hop mechanism, which is characterized by low migration barriers (~1 eV),[3] can be compared to the Ni-ASB mechanism in that Al transport by this mechanism is greatly enhanced once a percolating network of Ni vacancies is established as illustrated in Fig. 1(i). While the kinetic Monte Carlo simulations predict a high frequency for this mechanism, the alloy composition is likely not Al rich enough for a sufficiently high Ni-vacancy concentration required to form percolating networks.[27] Most of the pair-atom hops involving two Al atoms are therefore back and forth hops and do not contribute much to macroscopic Al transport. Hence, at the Al-rich composition considered here, Ni and Al diffusions rely primarily on the 6JC mechanism.

The above results clearly demonstrate a remarkable complexity of atomic diffusion in metallic alloys even for compounds such as $B2$-NiAl with its simple $B2$ crystal structure.

The decomposition of atomic transport into various hop mechanisms, as illustrated in Fig. 3, shows the tremendous sensitivity of the dominant diffusion mechanism to small changes in bulk alloy concentration. Contrary to expectation, a large fraction of hops in this intermetallic compound is mediated by simultaneous pair-atom hops. This understanding is not only intriguing from a scientific point of view, but is also of relevance from an engineering standpoint as strategies to alter diffusion behavior in $B2$-NiAl through alloying will depend sensitively on composition and the degree of local disorder.

We are grateful for financial support from NSF Grants No. DMR-0748516 and No. DMR-0605700.

APPENDIX

1. Total energies, migration barriers, and attempt frequencies

The calculations of total energies, migration barriers, and attempt frequencies were performed with DFT as implemented in the VASP plane-wave pseudopotential code within the generalized gradient approximation (Perdew-Wang 91).[19,20] The core-electron interaction was treated with the PAW method.[21,22] The nudged elastic band method was used to calculate migration barriers except for hops where the activated state is at a high symmetry point in which case only the energy of the activated and the end states of the hop were calculated. All calculations of migration barriers were performed in a 54-site supercell of $B2$-NiAl using a $3\times3\times3$ k-point mesh.

2. Kinetic Monte Carlo simulation methods

The kMC algorithm is based on the n-fold way method in which each hop is picked with probability $\Gamma_\xi/\Gamma_{\text{tot}}$, where Γ_ξ is the hop frequency of hop ξ and Γ_{tot} is the sum of all hop frequencies.[26] The time is updated after each hop by $-\ln \rho/\Gamma_{\text{tot}}$, where ρ is a random number between (0,1].[26] For each Ni vacancy, there are 86 possible hops and for each Al vacancy there are 38 possible hops. Tracer diffusion coefficients, $D_i^*=\langle\Sigma_\xi[\Delta\vec{R}_\xi^i(t)]^2\rangle/6tN_i$, at each composition were calculated within kMC simulations by averaging over trajectories, $\Delta\vec{R}_\xi^i(t)$, at different times and over simulations that started from different initial configurations (obtained with canonical Monte Carlo). A variety of alloy compositions were determined with grand canonical Monte Carlo simulations corresponding to an equilibrium vacancy concentration.[3] In the Ni-rich alloys, the MC cell contained 12^3 $B2$-NiAl unit cells (3456 sites) and 1000 kMC passes were performed (one kMC pass corresponds to each atom on average having performed a hop), starting from 100 initial configurations. In the Al-rich alloy an MC cell with 44^3 $B2$-NiAl unit cells (170 368 sites) was used and 60 kMC passes were performed starting from eight initial configurations. A significantly larger MC cell was required in the Al-rich alloy to obtain the correct equilibrium concentrations for antisite Al atoms, antisite Ni atoms, and Al vacancies. We ensured that our kMC cell sizes were sufficiently large and that the run times were long enough to guarantee that the average point-defect concentrations in the kMC runs were the same as predicted with grand canonical Monte Carlo simulations.[3]

3. Counting frequencies of hop mechanisms and sequences

Instead of counting the frequency of a hop sequence, we kept track of the total number of subhops for each sequence. Also, for a particular sequence, we combine the number of hops of different crystallographic types (e.g., we made no distinction between [110] 6JC, straight [100] 6JC, and bent [100] 6JC sequences when counting the number of hops involved in the 6JC).

The hops involved in the ASB-Ni sequence were counted by summing over NN Ni hops in the immediate vicinity of a Ni antisite. The first subhop of a triple-defect sequence is a Ni_{Al}-V_{Ni} hop in the vicinity of a V_{Ni} and is the reverse of the third V_{Al}-Ni_{Ni} subhop of the sequence (our results show that the numbers of these two subhops are almost identical). The second subhop is an Al_{Al}-V_{Al} NNN hop next to a Ni vacancy. We found that the second subhop is the bottleneck of the sequence as it occurs less frequently than the first and third hops. The number of hops involved in the triple-defect sequence was therefore taken as three times the number of Al_{Al}-V_{Al} NNN hops next to a Ni vacancy. The number of second subhops of the triple-defect sequence multiplied by 2 was subtracted from the first and third subhops and this difference was counted as NN Ni back and forth hops. Added to the number of NN Ni back and forth hops was the sum of Ni_{Al}-V_{Ni} and V_{Al}-Ni_{Ni} hops occurring in local environments other than those required by ASB-Ni and triple-defect sequence (which were found to be almost identical).

The NNN hops were counted directly, while the ASB-Al hops were determined by summing over all simultaneous pair hops involving two Al atoms not next to a Ni-antisite atom. The estimate of the 6JC mechanism was made by multiplying the second SPA hop of the sequence, involving two Al atoms next to a Ni-antisite atom, by 3 as this hop was found to be the bottleneck of the sequence.

[1] A. J. Bradley and A. Taylor, Proc. R. Soc. London, Ser. A **159**, 56 (1937).

[2] P. A. Korzhavyi, A. V. Ruban, A. Y. Lozovoi, Y. K. Vekilov, I. A. Abrikosov, and B. Johansson, Phys. Rev. B **61**, 6003 (2000).

[3] Q. Xu and A. Van der Ven, Intermetallics **17**, 319 (2009).

[4] E. W. Elcock and C. W. Mccombie, Phys. Rev. **109**, 605 (1958).

[5] G. F. Hancock and B. R. Mcdonnel, Phys. Status Solidi A **4**, 143 (1971).

[6] C. R. Kao and Y. A. Chang, Intermetallics **1**, 237 (1993).
[7] St. Frank, S. V. Divinski, U. Sodervall, and Chr. Herzig, Acta Mater. **49**, 1399 (2001).
[8] Y. Mishin, A. Y. Lozovoi, and A. Alavi, Phys. Rev. B **67**, 014201 (2003).
[9] A. Paul, A. A. Kodentsov, and F. J. J. Van Loo, J. Alloys Compd. **403**, 147 (2005).
[10] A. R. Allnatt and A. B. Lidiard, *Atomic Transport in Solids* (Cambridge University Press, Cambridge, 1993).
[11] A. Van der Ven and G. Ceder, Phys. Rev. Lett. **94**, 045901 (2005).
[12] A. Van der Ven, H. C. Yu, G. Ceder, and K. Thornton, Prog. Mater. Sci. **55**, 61 (2010).
[13] L. K. Moleko, A. R. Allnatt, and E. L. Allnatt, Philos. Mag. A **59**, 141 (1989).
[14] J. R. Manning, Phys. Rev. B **4**, 1111 (1971).
[15] I. V. Belova and G. E. Murch, Philos. Mag. A **80**, 599 (2000).
[16] A. Van der Ven, G. Ceder, M. Asta, and P. D. Tepesch, Phys. Rev. B **64**, 184307 (2001).
[17] A. Van der Ven, J. C. Thomas, Q. Xu, B. Swoboda, and D. Morgan, Phys. Rev. B **78**, 104306 (2008).
[18] J. M. Sanchez, F. Ducastelle, and D. Gratias, Physica A **128**, 334 (1984).
[19] G. Kresse and J. Furthmuller, Phys. Rev. B **54**, 11169 (1996).
[20] G. Kresse and J. Furthmuller, Comput. Mater. Sci. **6**, 15 (1996).
[21] P. E. Blochl, Phys. Rev. B **50**, 17953 (1994).
[22] G. Kresse and D. Joubert, Phys. Rev. B **59**, 1758 (1999).
[23] K. A. Marino and E. A. Carter, Phys. Rev. B **78**, 184105 (2008).
[24] G. H. Vineyard, J. Phys. Chem. Solids **3**, 121 (1957).
[25] R. LeSar, R. Najafabadi, and D. J. Srolovitz, Phys. Rev. Lett. **63**, 624 (1989).
[26] A. B. Bortz, M. H. Kalos, and J. L. Lebowitz, J. Comput. Phys. **17**, 10 (1975).
[27] I. V. Belova and G. E. Murch, Intermetallics **6**, 115 (1998).